Space-Based Visible End of Life Experiments

Joseph Scott Stuart
MIT Lincoln Laboratory
Andrew J. Wiseman
MIT Lincoln Laboratory
Jayant Sharma
MIT Lincoln Laboratory

ABSTRACT

The Space-Based Visible (SBV) sensor was launched to orbit on 24 April 1996 as part of the Midcourse Space Experiment (MSX) satellite. As the only optical space surveillance sensor in space, it has provided a unique space surveillance capability and has paved the way for future systems such as SBSS. After more than 12 years of operations, SBV and the MSX satellite are being permanently shut down by June 2008. This provides a unique opportunity to perform several experiments that were deemed too risky during SBV's operational lifetime. These experiments will be conducted through May 2008. Depending on spacecraft performance we plan to conduct several tests of advanced space situational awareness data collection modes including reduced target motion data collection for geosynchronous targets, high phase angle observations of geosynchronous targets, and discrimination of closely-spaced geosynchronous targets.

We also plan several experiments for sensor characterization that will yield insight into how the instrument has been affected by 12 years in low altitude orbit. These include observing well calibrated star fields to assess CCD sensitivity and charge transfer efficiency degradation, and Earth and moon limb observations to assess stray light rejection and optical cleanliness. We will also attempt to close the telescope cover, a procedure that has not been performed since 1998 due to fears that the cover may not reopen. If the cover successfully closes, we will acquire dark current and flat field data to compare with historical values for this sensor and we will acquire data during transit through the South Atlantic Anomaly to characterize the interaction between the focal plane and high-energy particles. Finally, we will attempt to warm the focal plane to determine whether annealing will improve the charge transfer efficiency that has significantly degraded since launch due to damage from high-energy protons.

1. Introduction

The Midcourse Space Experiment (MSX) satellite was launched in 1996 into an 898-km altitude, nearly sun-synchronous orbit [1]. One of the primary sensors aboard MSX was the Space-Based Visible (SBV) sensor, which was designed, built, and operated at MIT Lincoln Laboratory [2,3]. The SBV program had many goals including the demonstration of major new technologies (high off-axis rejection optics, advanced staring focal-plane arrays, onboard signal processing), the demonstration of space-based space surveillance techniques, and support of ballistic missile defense tests. After the primary mission of the MSX, the SBV sensor was transitioned from an experimental sensor to a full Contributing Sensor within the US Air Force Space-Surveillance Network (SSN), in April 1998. For 10 years SBV proved to be a valuable component of the SSN.

In early 2008, it became clear that the MSX spacecraft was close to complete failure. At that point, the primary on-board gyroscope used to maintain continuous fine attitude control had already failed, and the remaining gyroscope was showing symptoms of being near to failure. The failure of the last gyroscope would have rendered the spacecraft unable to maintain attitude control sufficient for operations. In addition, several course sensors had also failed. The MSX does not possess a de-orbiting capability. Also, the spacecraft has pressurized batteries which could overcharge and explode, creating a debris cloud that could endanger other spacecraft. Therefore, the decision was made to drain the batteries, shut down the spacecraft, and place it into the safest possible configuration before shutting down communications. The final shutdown sequence was executed in early June 2008.

Prior to final shutdown, time was made available during May and April 2008 to collect data with the SBV. These experiments included spacecraft operations that had been deemed too risky for a contributing sensor. The

experiments had two overarching goals. One was to demonstrate new data collection techniques for future space surveillance sensors such as the Space Based Space Surveillance (SBSS) Pathfinder system and to evaluate the Optical Processing Architecture at Lincoln (OPAL) platform. The other was to characterize the state of the SBV sensor to learn more about how the low altitude space environment has degraded the instrument.

Three separate types of experiments were scheduled to test new data collection techniques for future space surveillance sensors. One experiment is a geometry optimized search strategy for target satellites in geosynchronous Orbits. It uses the combined motion of the sensor and target to reduce the apparent angular velocity of the target on the focal plane allowing for longer integration times and greater sensitivity. Another experiment collected observations of target satellites at very high phase angles. This data will be used to better determine the relationship between brightness and phase angle to allow for better scheduling of space surveillance data collection. A third experiment was to collect images of tightly clustered targets in the geosynchronous belt to provide test data for advanced techniques for discrimination of closely spaced targets (CSOs). Finally, data was collected in ephemeris track mode. The results of these experiments will be the subject of future papers and will not be further covered here.

Several types of data were collected in order to characterize the state of the SBV sensor after 12 years in orbit. The Landolt star field SA-97 [4] was targeted to assess the system throughput and sensitivity on April 16. The moon limb and Earth limb were imaged on May 22 and May 24 to assess stray light rejection and optical cleanliness. Dark current data with the cover closed were collected on May 28. Closing the cover was deemed a high risk operation due to the possibility that the cover would not open again. Indeed, prior to this experiment, the cover had not been closed, and no dark current data collected since April 2000. Despite the many years of disuse, the camera cover did successfully close, dark data were collected, the cover was evaluated for light leakage, and the cover successfully re-opened. After the cover reopened, the focal plane cooler was turned off to allow the focal plane to reach ambient temperature and on May 29 the focal plane was further warmed by pointing the sensor at the hard Earth to test whether an annealing process could repair some of the silicon defects that have accrued due to radiation damage. After the focal plane warming process, the focal plane cooler was turned back on. Finally the pyrotechnic bolts that act as a backup focal plane cover release mechanism were successfully tested.

Day(s)	Experiment	Number of Events
46-52	Ephemeris Tracking	6
99, 101, 130	GEOST	3
107	Landolt	1
116, 137	Closely Spaced Objects	2
121, 123, 135	Metric Calibration	3
128	Modeling (EO-1)	1
142	High Phase Track	1
145	Earth Limb (NRER)	1
141	Moon Limb	1
149	Close Cover	1
149, 151	Dark Current	2
151	Annealing	1
151	Open Cover	1
151	Emergency Cover Open	1

Table 1. SBV End of Life Experiments.

2. Results

Annealing Test
The thermocouples that measure the temperature of the SBV imaging devices have been inoperable for some time. Therefore, the focal plane temperatures reached during the annealing test are not accurately known. Repair of radiation-induced damage in CCDs has been demonstrated on the Hubble Space Telescope [5] by heating the CCDs

to +30C for approximately 4 hours. In this one-time test with SBV, no improvement was noted in hot pixels, or charge transfer efficiency after the focal plane warm up. However, it was impossible to determine the temperature that the focal plane reached.

Dark Current

Analyzing the results of the dark current data collection presents several difficulties. As mentioned in the results of the annealing test, the focal plane temperature readings are not available for SBV. The spacecraft was commanded to maintain the sensor at the normal operational temperature of -40C. The amount of power being used by the focal plane cooler was monitored during the data collection and remained at normal levels throughout, indicating a high likelihood that the sensor was at the commanded temperature. Time was not available to collect dark current data at different operating temperatures. In pre-flight laboratory tests, dark current was found to double for each 6 degrees C, so a fairly small change in the operating temperature could be the cause of any differences between the end of life dark current values and the pre-flight and initial on-orbit checkout values.

Another problem with analyzing the dark current data was that time and operational constraints did not allow for the collection of dark current data at more than one integration time and gain. The standard integration time of 0.625 seconds and low gain were used. Having data at only a single integration time makes it difficult to separate out the dark current from the readout noise. The readout electronics for the SBV sensor has two gain settings of approximately 6 electrons per digital number (e^-/DN) and 24 e^-/DN. Most of the initial on-orbit characterization data were taken at the high gain setting, but most operational space surveillance data is taken at the low gain. For the end of life characterization, an attempt was made to collect dark current data at both gain settings, but data were actually acquired for only the low gain setting. Combined with the short integration, the gain setting of the 24 e^-/DN makes it difficult to accurately measure dark current. One final problem in analyzing the dark current data is due to the measurement precision of the bias voltage level for the analog to digital converters. This bias level is recorded for each image, but is only reported accurate to one digital number

To process the dark current data, the raw frames were separated into groups according to which CCD they were from. There is no dark current data available for CCD #4. In all images, normal levels were near 20 counts with a small number of hot pixels, cold pixels, and multi-pixel radiation events. To clean these spurious signals from the dark data, each image was first cleaned of obviously bad pixels (those with counts below 10 or above 1000 out of a possible 4096, the limit of the 12-bit AD converters). Next, a mean and standard deviation was computed from the remaining pixels in the image, and pixels more than 1-sigma below the mean or more than 4-sigma above the mean were eliminated. This typically resulted in fewer than 100 pixels per 420x420 image being eliminated. There was 1 very noisy image in which almost 10% of the pixels were eliminated and that image was removed from the data set. After eliminating bad pixels, the mean and variance of the remaining pixels was computed. The reported bias voltage level was subtracted from the mean.

At this point in the processing, the dark current levels are expressed in DNs. To convert them to e^-/s, we divide by the integration time (0.625 seconds) and multiply by the gain (24 e^-/DN). Table 2 gives the resulting values. As can be seen in the table, the dark current is higher than the pre-flight and initial on-orbit checkout value of 18 e^-/s. This is probably due to degradation of the CCD from exposure to radiation. There is also the possibility that the focal plane was slightly warmer than expected. Finally, there were measurement issues with the gain and bias levels.

CCD#	Bias Voltage (DNs)	Mean (counts)	Dark Current (e^-/s)
1	16	18.75	105.6
2	18	19.92	73.7
3	20	21.69	64.9

Table 2. Computed dark current from SBV end of life data. Dark current data was collected from a large number (~100) of full frame dark images for each of three CCDs. After cleaning bad pixels and radiation events from each image, a bias-subtracted mean is calculated. Finally, an estimate of the dark current is computed using the integration time and estimated system gain. The dark current is higher than the pre-flight and initial on-orbit check out values of 18 e^-/s, as would be expected.

Charge Transfer Efficiency

CCD imagers used in space become damaged due to collisions with energetic particles and photons [8]. One of the results of radiation damage is loss of charge transfer efficiency. Reduced charge transfer efficiency produces images in which the signal from point sources is smeared out into a "charge tail" along the read out direction (columns) of the CCD, Fig. 1.
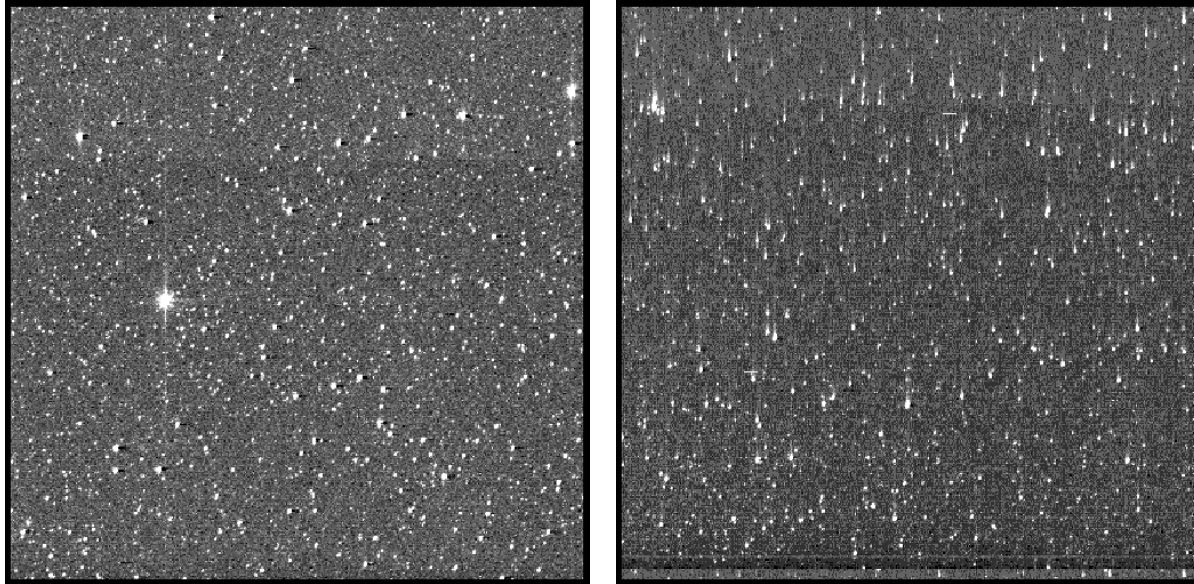

Figure 1. Illustration of reduced charge transfer efficiency in SBV images due to damage from radiation exposure. The left image is from Aug 1996 and shows good charge transfer efficiency with round looking stars. The image on the right is from Jan 2001 and shows degraded charge transfer efficiency appearing as "charge tails" in the column direction for stars.

To characterize the extent of the charge transfer efficiency degradation after 10 years on orbit, the shapes of the stars were measured with 2-D elliptical Gaussians in which the ellipticity was constrained to lie along the columns of the images. A sequence of star-field images from Aug 1996, and a sequence of star-field images from the end of life data in May 2008 were both measured in the same way. All stars with signals levels more than 10 times the background noise level were extracted and a restricted 2-D elliptical Gaussian was fit to each star. The 1-sigma width of the Gaussian point spread function in the row (or across-column) direction and the column direction was saved. If the star profiles tend to be larger in the column direction, this is evidence of smearing in the readout direction and of decreased charge transfer efficiency. For the 1996 data, 2026 stars were measured, and for the May 2008 data, 1646 stars were measured. Fig. 2 shows a scatter plot of the resulting row widths versus the column widths for both data sets, with outliers removed. The line plotted indicates where stars would fall if the widths are equal in the two directions. Points that fall above the line are elongated in the column direction. Clearly, the 1996 imagery shows very little tendency for the stars to be elongated in the column direction which is indicative of minimal degradation of the charge transfer efficiency at the beginning of on-orbit operations. The data from 2008, however, shows that stars are systematically elongated in the column direction indicating substantial degradation of charge transfer efficiency.
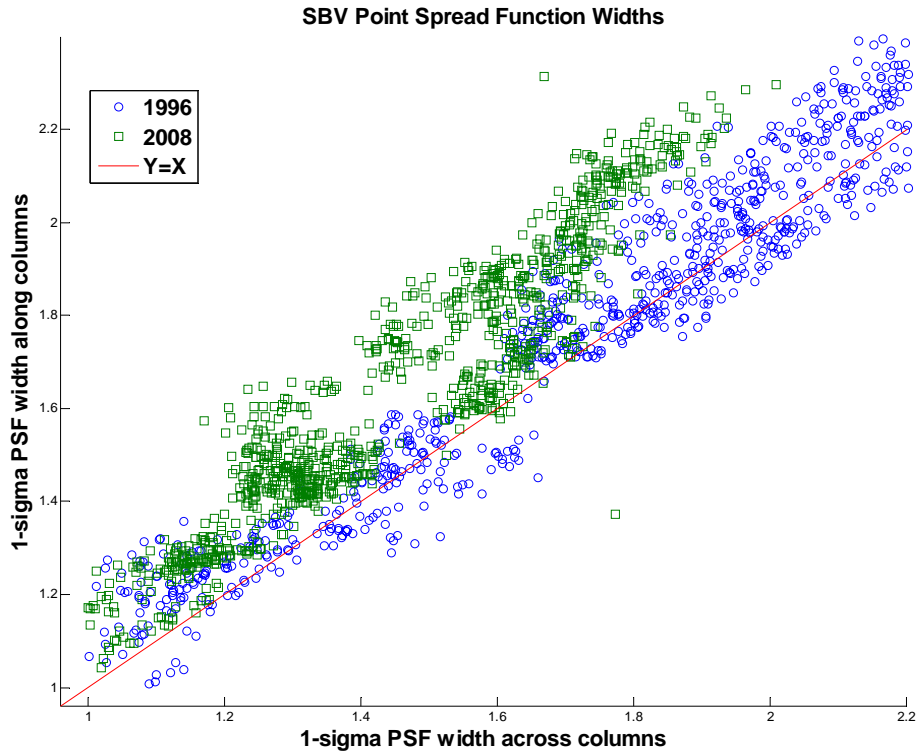
SBV Point Spread Function Widths

Fig. 2. Charge Transfer Efficiency Degradation for SBV from 10 years of exposure to radiation on-orbit. Gaussian profile fitting was used to measure the widths of stars in images from 1996 and 2008. The 2008 data shows substantial elongation of stellar profiles in the column or readout direction compared to the across-column or row direction. The 1996 data shows that the across column and along column directions are virtually the same in terms of stellar profile width. This is indicative of degradation of charge transfer efficiency.

The same stellar profile widths are shown in Fig. 3 as histograms. In the across column or row direction the point spread function has not changed substantially between 1996 and 2008. However the ratio of the row widths to the column widths is substantially larger in the 2008 images, a clear indication of charge transfer efficiency degradation. The ratio of Gaussian point spread function widths is difficult to convert to a value for the charge transfer efficiency, but analysis is ongoing to determine the actual charge transfer efficiency value from other measurements of the end of life data.
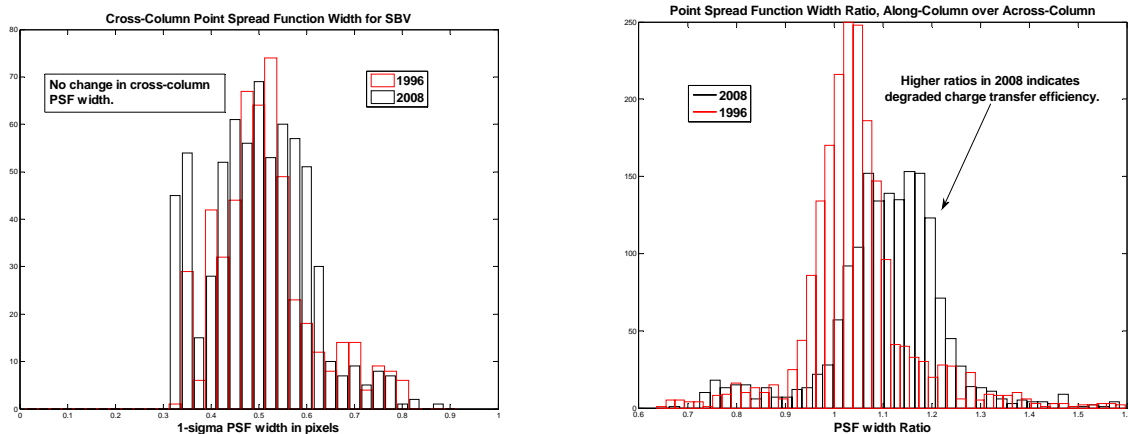

Fig. 3. Charge Transfer Efficiency Degradation for SBV from 10 years of exposure to radiation on-orbit. Gaussian profile fitting was used to measure the widths of stars in images from 1996 and 2008. The left plot shows

a histogram of the stellar profile widths in the across track direction. There is little change between the 1996 and 2008 data indicating no overall degradation in the size of the point spread function over the lifetime of the sensor. The right plot shows a histogram of the ratio of the stellar profile width in the column direction divided by the stellar profile width across columns. The shift toward higher ratios in the 2008 data relative to 1996 is clearly shows degradation of charge transfer efficiency.

3.   Conclusions and Future Work

Much work remains to be done to fully analyze the SBV end of life experiments. Initial conclusions described here are that the dark current for the sensor remains fairly close to the pre-flight value of 18 e⁻/s, though the lack of a temperature reading for the sensor and problems during the end of life data collection make a definitive conclusion difficult. The charge transfer efficiency has clearly degraded substantially over the 12 years of SBV's on-orbit life. Work remains to determine more precisely the charge transfer efficiency of the CCDs. In addition to continuing to investigate the dark current and charge transfer efficiency, work is also ongoing to evaluate several other aspects of the sensor. Data were collected with the sensor pointing near the Earth and near the illuminated limb of the moon in order to evaluate telescopes the stray light rejection capabilities and assess the level of cleanliness of the optics. Similar comparison data are available from early in the mission to determine the degree of degradation while on-orbit. Images of standard stellar fields for photometric calibration were collected. When compared with similar measurements taken immediately after launch, this will address degradation of the total system throughput which is a combination of the optical throughput and the CCD's quantum efficiency. The SBV end of life data collection event was a unique opportunity to characterize a valuable sensor after 12 years in orbit and much work remains to be done to understand the implications for future space-based systems.

4.   REFERENCES

1. Mill, J.D., O'Neill, R.R., Price, S., Romick, G.J., Uly, O.M., and Gaposchkin, E.M., *Midcourse Space Experiment: Introduction to the Spacecraft, Instrucments, and Scientific Objectives*, JOURNAL OF SPACECRAFT AND ROCKETS, Vol 31(5), 900-907, 1994.
2. Stokes, G.H., von Braun, C., Sridharan, S., Harrison, D., Sharma, J., *The Space-Based Visible Program*, Lincoln Laboratory Journal, Vol. 11(2), 205-238, 1998.
3. Sharma, J., Stokes, G.H., von Braun, C., Zollinger, G., Wiseman, A., *Toward Operational Space-Based Space Surveillance*, Lincoln Laboratory Journal, Vol. 13(2), 1-26, 2002.
4. Landolt, A.U., *UBVRI Photometric Standard Stars in the Magnitude Range 11.5<V<16.0 Around the Celestial Equator*, AJ 104-1, 340-491, 1992.
5. Polidan, E.J., et al., *A study of hot pixel annealing in the Hubble Space Telescope Wide Field Camera 3 CCDs*, Proc. SPIE, Vol. 5487, 289, 2004.
6. Barth, A. J., in ASP Conf. Ser., Vol. 238, *Astronomical Data Analysis Software and Systems X*, eds. F. R. Harnden, Jr., F. A. Primini, & H. E. Payne (San Francisco: ASP), 385, 2001, and on the website http://www.physics.uci.edu/~barth/atv/
7. IDL Astronomy User's Library, http://idlastro.gsfc.nasa.gov/contents.html
8. Janesick, J. and Elliot, T., *History and Advancements of Large Area Array Scientific CCD Imagers*, ASTRONOMICAL CCD OBSERVINGS AND REDUCTION TECHNIQUES, ed. S. Howell, Astronomical Society of the Pacific Conference Series Vol 23.